Materials Research Proceedings 41 (2024) 1955-1961 https://doi.org/10.21741/9781644903131-216

# Study of cutting force in milling of aluminum-lithium alloy

TAMURA Shoichi[1,a *], MORII Daisuke[1,b] and MATSUMURA Takashi[1,c]

[1]Tokyo Denki University, 5 Senjyu Asahi-cho, Adachi-ku, Tokyo, 120-8551, JAPAN

[a]tamuras@mail.dendai.ac.jp, [b]22kmk28@ms.dendai.ac.jp, [c]tmatsumu@cck.dendai.ac.jp

**Keywords:** Milling, Aluminum-Lithium Alloy, Cutting Force

**Abstract.** Aluminum-lithium alloy has been applied to aircraft parts for reduction of the fuel consumption with its high specific strength. Cutting tests are performed to characterize the cutting force of aluminum-lithium alloy (Constellium, 2098-T8) and conventional extra-super duralumin (JIS A7075-T6) in slot milling at different spindle speeds. When the cutting speed increases, the tangential and radial components in cutting force of the aluminum-lithium alloy considerably decrease up to 300 m/min; while those of A7075 decrease monotonically. Then, the cutting process of aluminum-lithium alloy is discussed in an energy-minimum cutting force model. The shear angle and the friction angle increase with the cutting velocity, and the shear stress on the shear plane decreases with the increase of cutting velocity. According to the cutting model in milling of aluminum-lithium alloy, the cutting velocity should be taken higher than 300 m/min to not only reduce the cutting force but also control the surface finish.

## Introduction

Aluminum-lithium alloy has been attracted in aerospace industry due to its lightweight and high strength, where adding 1 wt% lithium to aluminum reduces the density by 3% and enhances the elastic modulus by 6% [1]. Aluminum-lithium alloys recently have been applied to the parts used in not only military but also commercial aircrafts [1]. Therefore, high quality is required for cutting of aluminum-lithium alloy as well as high production rate.

J. Niu et al. [2] studied the corrosion resistance on the machined surface in milling of aluminum-lithium alloy 2A97 under dry cutting conditions. According to their discussion, a larger strain hardening occurs in subsurface formed by cutting than that of grinding or polishing. The machined surface in milling promotes the corrosion resistance with the strain hardening. H. Mu et al. [3] compared the surface integrity in face milling of aluminum-lithium alloy with air coolant and with liquid nitrogen. Liquid nitrogen efficiently induces compressive residual stress. Furthermore, residual stress was associated with the spindle speed, the depth of cut, the feed rate, and the feed direction with respect to the rolling direction, in regression analysis. J. Niu et al. [4] discussed characteristics of machined surface in milling of aluminum-lithium alloy for the cutting parameters. As the cutting velocity increases, they demonstrated that the effect of thermal softening suppresses the work hardening. Denkena et al. [5] discussed the effect of the sharpness of cutting edge on the stability in cutting process with the temperature rise in peripheral milling of Al-Li 2196. Although the cutting process of aluminum-lithium alloys has been studied so far, the cutting force has not been yet discussed in terms of the cutting model.

This paper discusses the cutting processes of aluminum-lithium alloy in milling. First, the cutting forces in milling of aluminum-lithium alloy are measured and compared to those of A7075 to discuss the effect of cutting velocity. Then, the cutting force is analyzed in an energy-minimum cutting force model, where the orthogonal cutting data used in the model are identified with referring to the actual cutting forces. The change in the cutting model is associated with the chip morphology and adhesion, which are related to the shear deformation for chip formation and the friction on the rake face, respectively.

## Cutting Test

The cutting tests in milling of grooves were conducted on a 3-axis vertical machining center (Makino, V33i), as shown in Fig. 1. 4 mm thick plates of aluminum-lithium alloy (Constellium, 2098-T8) and conventional extra-super duralumin (JIS A7075-T6) were employed in the cutting tests. The aluminum-lithium alloy and the conventional extra-super duralumin are hereinafter referred to as Al-Li2098 and A7075 in the paper. Measured hardness of Al-Li2098 was 170 HV, which was nearly the same as 168 HV of A7075 each other.

The workpiece was clamped on a piezoelectric dynamometer (Kisler, 9256C2) mounted on the machine table to measure the cutting force. The cutting force was acquired at 100 kHz. A carbide two-flute square end mill coated with a Cr-based thin layer was used in the cutting test. The tool diameter and the helix angle were 12 mm and 30°, respectively. The end mill was clamped to the spindle of machine tool with a collet chuck. The end mill was fed along X direction in slotting in an axial depth of cut of 2 mm, as shown in Table 1. In investigation of the effects of cutting velocity on the cutting force, the spindle speed was controlled in a range of cutting velocity from 60 to 600 m/min, where the feed rate was constant at 0.04 mm/tooth. The chip thickness and the surface finish were measured with an optical microscope (Keyence, VHX-2000) and a laser microscope (Keyence, VK-X100).

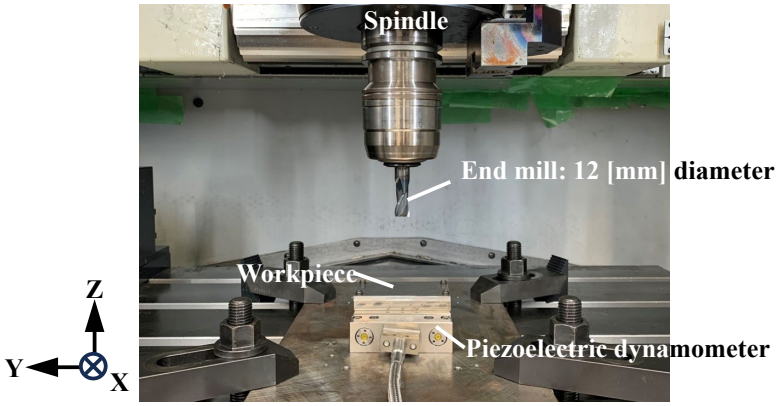


*Fig. 1 Cutting test in peripheral milling*

*Table 1 Cutting conditions*

| | |
|---|---|
| Axial depth of cut [mm] | 2 |
| Gloove width [mm] | 12 |
| Cutting velocity [m/min] | 60, 180, 300, 450, 600 |
| Feed rate [mm/tooth] | 0.04 |
| Lubrication | Dry |

## Cutting Force in Milling

Figure 2 shows the measured cutting forces in milling of Ai-Li2098 at a cutting velocity of 60 m/min, where the cutting force are designated as the load applied to the tool. The cutting force changes periodically in half of the cutter rotation cycle of 0.019 s from a time of O to O' in Fig.2.

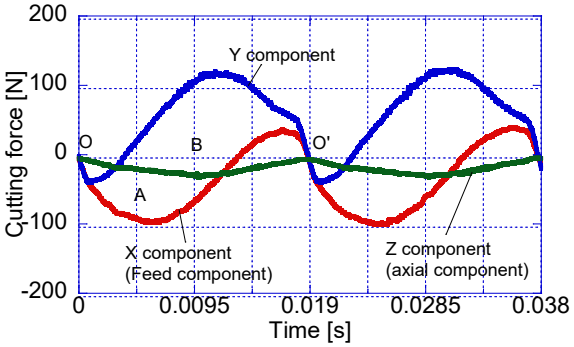


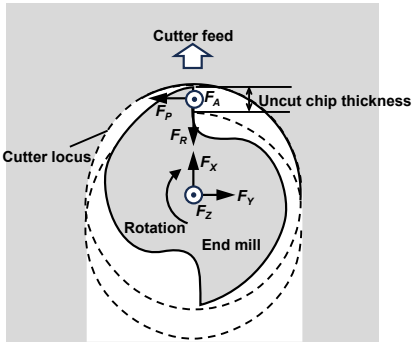


*Fig. 2 Cutting force measurement* *Fig. 3 Cutting force at the maxmum uncut chip thickness*

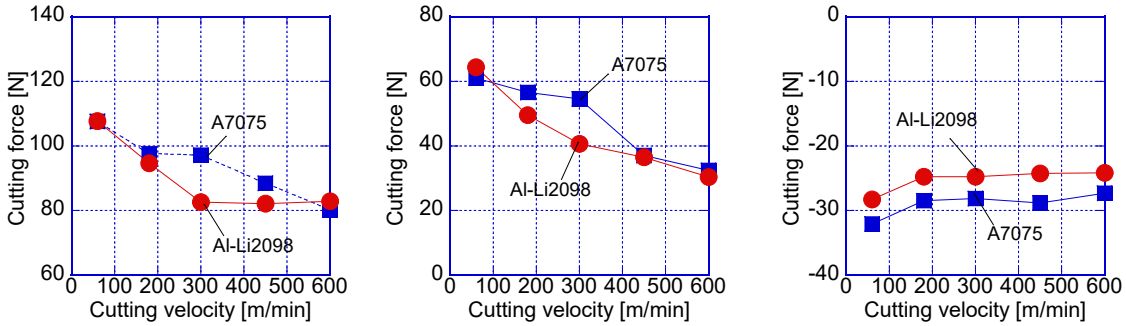


(a) Principal component (b) Radial component (c) Axial component

*Fig. 4 Cutting force components with cutting velocity*

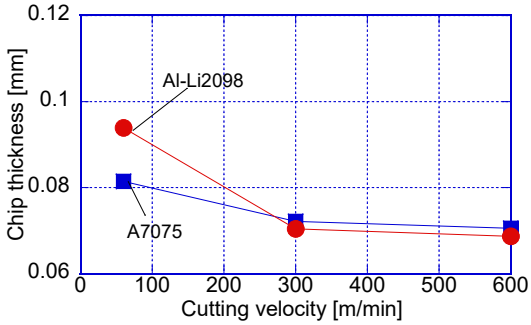


*Fig. 5 Chip thickness*

Because the cutting force components of a rotating edge change periodically with not only the uncut chip thickness but also the cutting direction in the measurement coordinate system of dynamometer, as shown in Fig. 3 viewed from upside of tool. The cutting force changes as follows:

1) At a time of O, an edge engages in the workpiece, and another edge exits from the workpiece. Because the uncut chip thickness is small around 0 s, little cutting force components were measured. Because the cutting direction nearly coincides with +X direction just after engagement. The negative X and Z components in the cutting force increase with the uncut chip thickness.
2) From A to B, the cutting direction turns gradually to Y direction from X direction. Then, X component decreases; while Y component, in turn, increases with cutter rotation, respectively.
3) When the cutting direction is oriented to -Y direction at the maximum uncut chip thickness at B, Y component loaded on the tool becomes large.
4) From B to O', the cutting force components decreases with the uncut chip thickness.

Materials Research Proceedings 41 (2024) 1955-1961 https://doi.org/10.21741/9781644903131-216

In Fig. 3, X, Y, and Z components ($F_X$, $F_Y$, and $F_Z$) in the measurement coordinate system are directly regarded as radial, tangential, and axial components ($F_R$, $F_P$ and $F_A$) loaded on the rotating edge at B. Fig. 4 shows force components at B in the coordinate system of rotating edge for the cutting velocities, where the measured components are averaged in 5 or more rotations. The cutting force components becomes small at high cutting velocities. The principal and the radial components in milling of Ai-Li2098 decrease significantly up to 300 m/min; and then, the changing rates become small up to 600 m/min. Those of A7075 decrease monotonically up to 600 m/min. The axial components of Al-Li2098 are smaller in all cutting velocities than those of A7075. These results will be discussed in the next section with an analytical force model.

Fig. 5 shows the maximum chip thicknesses at cutting velocities of 60, 300, and 600 m/min. Because the chip thickness becomes small at higher cutting velocities, the shear angle increases with the cutting speed in the shear plane cutting model.

**Analytical Force Model**

An energy force model was applied to characterize the cutting process in slot milling of Al-Li2098. The force model in milling was presented in Reference [6]. The force model is briefly described here. A three-dimensional chip flow in milling is interpreted as a piling up of the orthogonal cuttings in the planes containing the cutting velocities $V$ and the chip flow velocities $V_c$, as shown in Fig. 6. Although plastic deformation occurs in the chip formation, the interaction between each orthogonal cutting plane is ignored on the assumption that a rigid chip flows at an angular velocity. The orthogonal cutting models are given by the following equations:

$$\left.\begin{aligned} \phi &= \exp(A_{00}V + A_{01}t_1 + A_{02}\alpha + A_{03}) \\ \tau_s &= \exp(A_{10}V + A_{11}t_1 + A_{12}\alpha + A_{13}) \\ \beta &= \exp(A_{20}V + A_{21}t_1 + A_{22}\alpha + A_{23}) \end{aligned}\right\} \quad (1)$$

where $\phi$, $\tau_s$ and $\beta$ are the shear angle, the shear stress on the shear plane, and the friction angle, respectively. $V$, $t_1$, and $\alpha$ are the rake angle, the cutting velocity, and the uncut chip thickness in the orthogonal cutting. $A_{ij}$ ($i$ = 0,1,2; $j$ = 0,1,2,3) are parameters acquired in the orthogonal cutting tests. $A_{ij}$ can also be identified or refined with referring to the actual cutting force in milling by inverse analysis [7]. The chip formation is controlled by the first equation of Eq. (1). Machinability of workpiece may be evaluated by the second equation. Friction of the tool-chip interface was characterized by the friction angle in the third equation. Because the cutting temperature is associated with the cutting speed, the thermal effect on material behavior is predominantly

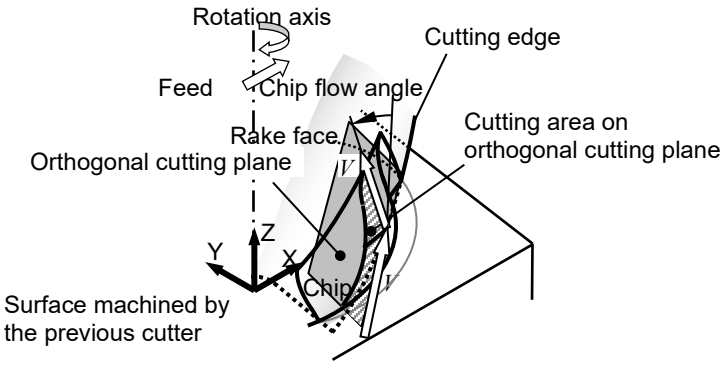


*Fig. 6 Chip flow model in milling*

controlled by $A_{i0}$ ($(i = 0,1,2)$ in each equation. Based on the measured cutting forces in the range of cutting velocity from 60 to 300 m/min, the orthogonal cutting data were acquired as:

Al-Li2098:

$$\left.\begin{aligned}\phi &= \exp(0.07092V + 7976t_1 + 0.005507\alpha - 1.215)\\ \tau_s &= \exp(-0.05393V - 1946t_1 + 0.25596\alpha + 19.95)\\ \beta &= \exp(0.00608V - 316.2t_1 + 0.09937\alpha - 0.4774)\end{aligned}\right\} \quad (2)$$

A7075:

$$\left.\begin{aligned}\phi &= \exp(0.02509V + 7840t_1 + 0.005507\alpha - 1.010)\\ \tau_s &= \exp(-0.03950V - 1688t_1 + 0.1317\alpha + 20.03)\\ \beta &= \exp(0.04458V - 557.9t_1 + 0.02515\alpha - 0.6493)\end{aligned}\right\} \quad (3)$$

Figure 7 compares the simulated and the measured cutting forces in milling of Al-Li2098 and A7075 at cutting velocities of 60 and 300 m/min. The force model and the orthogonal cutting data are verified in the agreement of the simulated cutting forces with the measured ones.

**Change in Cutting Model**

The cutting model at the center of cutting area is discussed in the range of cutting velocities from 60 to 300 m/min. Figure 8 shows the shear angles, the shear stress on the shear plane, and the friction angle in the cutting model. The shear angle increases with the cutting velocity in Fig. 8(a). In milling of Al-Li2098, the shear angle is more sensitive to the cutting velocity than that of A7075, where the sensitivity to cutting velocity is controlled by $A_{00}$ in Eq. (1). Since the shear force reduces with the shear plane at a large shear angle, the cutting force components are considerably reduced with increasing the cutting velocity shown in Fig. 4.

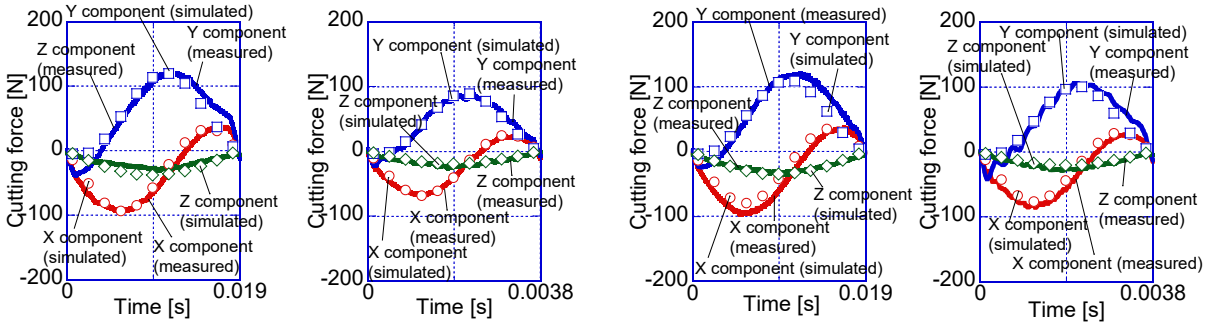


(a) 60 m/min (Al-Li2098) (b) 300 m/min (Al-Li2098) (c) 60 m/min (A7075) (d) 300 m/min (A7075)

*Fig. 7 Cutting force simulation*

Then, the shear stress on the shear plane becomes small at high cutting velocities, as shown in Fig. 8(b). As the cutting temperature increases with the cutting velocity, the workpiece undergoes thermal softening at high cutting velocities, which reduces the shear stress on the shear plane.

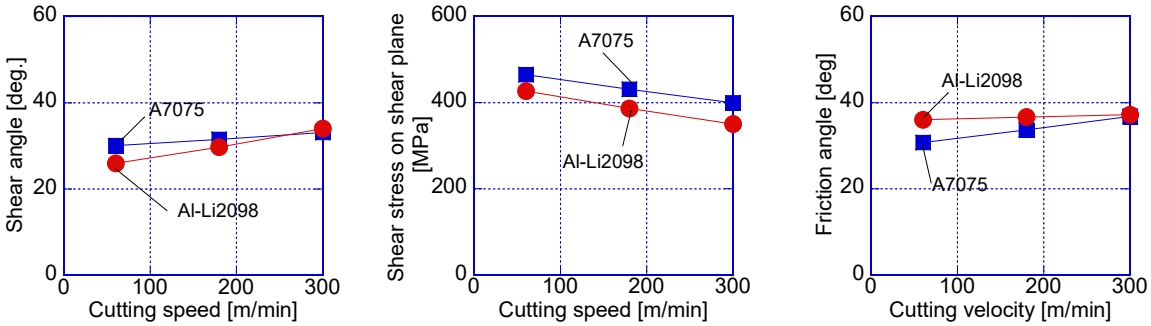


(a) Shear angle (b) Shear stress on shear plane (c) Friction angle

*Fig. 8 Shear plane cutting model*

Although both materials have similar hardness at room temperature, the shear stress on the shear plane of Al-Li2098 remains consistently lower compared to A7075. Generally, aluminum lithium alloys have lower thermal conductivity than conventional aluminum alloys. Therefore, the cutting temperature of Al-Li2098 is expected to be higher than that of A7075. Then, the mechanical strength of Al-Li2098 decreases significantly with the temperature rise. The effect of cutting speed on the thermal softening is evaluated by $A_{10}$ in Eq. (1). The relatively large negative $A_{10}$ in Eq.(2) gives more contribution to reduction of the shear stress when the cutting velocity increases in milling of Al-Li2098.

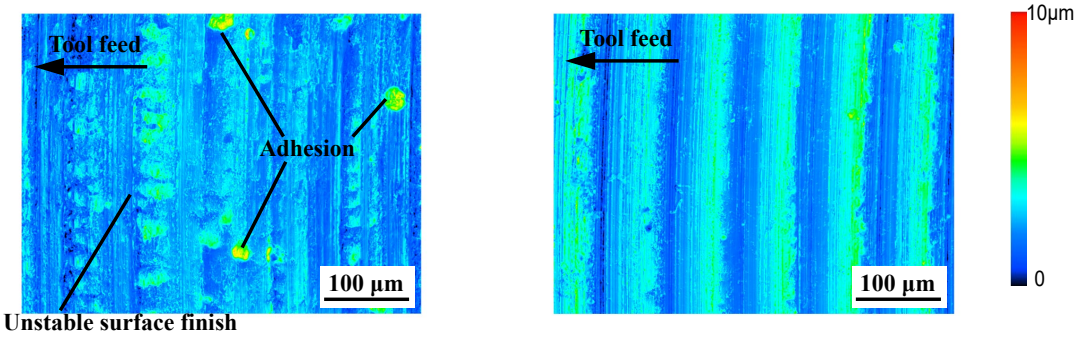


(a) Al-Li2098 (b) A7075

*Fig. 9 Height distribution on machined surface*

The friction angles of both materials increase with the cutting temperature due to activation of affinity in the interface between the thermal softened chip and the rake face, as shown in Fig. 8(c). Although the friction angles at 300 m/min are similar in both materials, the angles of Al-Li2098 indicate larger angles in comparison to that of A7075 at cutting velocities of 60 and 180 m/min. Fig. 9 compares the height distributions on the surface finishes of Al-Li2098 and A7075 at a cutting velocity of 60 m/min. Some residual adhesions are observed on the unstable cutter marks in Fig. 9(a) of Al-Li2098; while regular cutter marks are formed in Fig. 9(b) of A7075. Although further investigation is required for the scientific discussion between adhesion and the friction, the large friction force of Al-Li2098 may promote adhesion and repeat growing and dropping of bult-up edges on the tool-chip interface at low cutting velocities. Adhesion of Al-Li2098 deteriorates the surface finish more than A7075.

According to the above discussions, the cutting velocity should be taken more than 300 m/min to finish fine surfaces with low cutting forces in milling of Al-Li2098.

## Summary

The paper has studied milling of Al-Li2089 in slotting to characterize the cutting force in terms of its sensitivity to cutting velocity. The cutting force is compared with A7075. The results are summarized as:

1) In milling of Al-Li2098, the cutting force components in tangential and radial directions at the maximum uncut chip thickness decrease significantly up to a cutting velocity of 300 m/min, while those of A7075 decrease monotonically up to a cutting force of 600 m/min.
2) Analytical cutting force model is applied to discuss the cutting process. Although the shear angle increases with the cutting velocity. The sensitivity of the shear angle of Al-Li2098 to the cutting velocity is larger than that of A7075. Therefore, the cutting force considerably reduce up to 300 m/min.
3) The shear stress on the shear plane of Al-Li2098 becomes small in all tested cutting velocity. Thermal softening of Al-Li 2098 may occur more at high cutting temperatures compared to that of A7075.
4) The friction angles become larger in milling of Al-Li2098 at low cutting velocities in comparison to those of A7075. The large friction force at low cutting velocity may induce growth of built-up edges on the rake face.

## References

[1] N. Eswara, P. R. J. H. Wanhill, Aerospace Materials and Material Technologies, Indian Institute of Metals Series 1, (2017).

[2] J. Niu, Z. Liu, B. Wang, Y. Hua, G. Wang, Effect of Machining-induced Surface Integrity on the Corrosion Behavior of Al–Li alloy 2A97 in Sodium Chloride Solution, Materials and Corrosion, 70, (2019), 2, 259-267. https://doi.org/10.1002/maco.201810380

[3] H. Mou, X. Huang, X. Zhang, H. Ding, Experimental Study of Surface Integrity of Aluminum Lithium Alloy by Face Milling, Intelligent Robotics and Applications 6th international conference ICIRA 2013 (2013), 25-28. https://doi.org/10.1007/978-3-642-40849-6_50

[4] J. Niu, Z. Liu, X. Ai, W. Huang, G. Wang, R. Duan, Characteristics of Machined Surface Integrity in Face Milling Al-Li Alloy 2A97 with Carbide Inserts, International Journal of Advanced Manufacturing Technology, 101 (2019), 1–4, 839–848. https://doi.org/10.1007/s00170-018-2907-8

[5] B. Denkena, J. Brüning, D. Niederwestberg, R. Grabowski, Influence of Machining Parameters on Heat Generation during Milling of Aluminum Alloys, Procedia CIRP, 46 (2016), pp. 39–42. https://doi.org/10.1016/j.procir.2016.03.192

[6] T. Matsumura, E. Usui, Predictive Cutting Force Model in Complex-shaped End Milling based on Minimum Cutting Energy, Int. J. Mach. Tools Manuf., 50 (2010), 5, 458–466. https://doi.org/10.1016/j.ijmachtools.2010.01.008

[7] T. Matsumura, T. Shirakashi, and E. Usui, Adaptive cutting force prediction in milling processes, International Journal of Automation Technology, 4 (2010), 3, 221–228https://doi.org/10.20965/ijat.2010.p0221